Journal of Geophysical Research: Planets

RESEARCH ARTICLE
10.1029/2018JE005747

Special Section:
5th International Planetary Dunes Workshop Special Issue

Patterns in Mobility and Modification of Middle- and High-Latitude Southern Hemisphere Dunes on Mars

Maria E. Banks[1,2,3], Lori K. Fenton[4], Nathan T. Bridges[5], Paul E. Geissler[6], Matthew Chojnacki[7], Kirby D. Runyon[5], Simone Silvestro[4,8], and James R. Zimbelman[2]

[1]NASA Goddard Space Flight Center, Greenbelt, Maryland, USA, [2]Center for Earth and Planetary Studies, Smithsonian National Air and Space Museum, Washington, District of Columbia, USA, [3]Planetary Science Institute, Tucson, Arizona, USA, [4]SETI Institute, Mountain View, California, USA, [5]Johns Hopkins University, Applied Physics Laboratory, Laurel, Maryland, USA, [6]U.S. Geological Survey, Flagstaff, Arizona, USA, [7]Lunar and Planetary Laboratory, University of Arizona, Tucson, Arizona, USA, [8]INAF Osservatorio Astronomico di Capodimonte, Naples, Italy

Abstract Change detection analyses of aeolian bedforms (dunes and ripples), using multitemporal images acquired by the Mars Reconnaissance Orbiter High Resolution Imaging Science Experiment (HiRISE), can reveal migration of bedforms on Mars. Here we investigated bedform *mobility* (evidence of wind-driven migration or activity), from analysis of HiRISE temporal image pairs, and dune field *modification* (i.e., apparent presence/lack of changes or degradation due to nonaeolian processes) through use of a dune stability index or SI (1–6; higher numbers indicating increasing evidence of stability/modification). Combining mobility data and SI for 70 dune fields south of 40°S latitude, we observed a clear trend of decreasing bedform mobility with increasing SI and latitude. Both dunes and ripples were more commonly active at lower latitudes, although some high-latitude ripples are migrating. Most dune fields with lower SIs (≤3) were found to be active while those with higher SIs were primarily found to be inactive. A shift in prevalence of active to apparently inactive bedforms and to dune fields with SI ≥ 2 occurs at ~60°S latitude, coincident with the edge of high concentrations of H_2O-equivalent hydrogen observed by the Mars Odyssey Neutron Spectrometer. This result is consistent with previous studies suggesting that stabilizing agents, such as ground ice, likely stabilize bedforms and limit sediment availability. Observations of active dune fields with morphologies indicative of stability (i.e., migrating ripples in SI = 3 dune fields) may have implications for episodic phases of reworking or dune building, and possibly geologically recent activation or stabilization corresponding to shifts in climate.

Plain Language Summary Dune fields and sand sheets, very similar to those we see on Earth, are observed on the surface of Mars. Their presence attests to the importance of wind-driven activity in shaping the Martian surface. Using repeated high-resolution imaging with the HiRISE (High Resolution Imaging Science Experiment) camera in orbit around Mars on the Mars Reconnaissance Orbiter spacecraft, we can now look closely at dunes and ripples (collectively referred to as bedforms) on Mars to find evidence of changes over time. Changes in or movement of the bedforms indicate where they are currently active and migrating across the surface. Actively migrating bedforms provide valuable information about present-day conditions on the surface such as sediment supply, wind speed, and wind direction. In this study, we investigated the activity of dunes and ripples in the middle and high latitudes of the southern hemisphere of Mars. We combined our results with those from investigations that looked at how the bedforms are degrading and being modified from nonwind-driven processes, indicative of dune inactivity. Our results show that dunes and ripples are progressively less active and show increasing evidence of degradation and erosion with proximity to the south pole. In the northern part of our study area (~40–55°S latitude), dune fields are mobile and are not degrading. Generally speaking, conditions where these dune fields formed, such as sediment supply and wind speeds, remain favorable for wind-driven activity today. In the high southern latitudes (> ~60°S), it appears that conditions favorable to dune field and sand sheet formation have shifted to less favorable conditions in most locations, perhaps episodically, since they originally formed. This shift in prevalence of active to apparently inactive bedforms and to dune fields that are more degraded occurs at roughly 60°S latitude and coincides with the edge of high concentrations of H_2O-equivalent hydrogen observed by the Mars Odyssey Neutron Spectrometer and interpreted to indicate ice beneath the surface. Our observations of decreasing bedform mobility with increasing latitude support the accumulation of ground ice between dune sand grains, which may be stabilizing the grains and reducing sand availability in present climate conditions. Some dunes may be stabilized by ground ice at their core, while surface/

Key Points:
- The mobility of dunes and ripples decreases with increasing latitude and degradation for southern hemisphere Martian dune fields
- A marked shift toward reduced bedform activity and widespread dune degradation begins poleward of ~60°S latitude
- Results support stabilization of sand sediments, likely by polar processes such as accumulating ground ice

Supporting Information:
- Supporting Information S1
- Table S1

Correspondence to:
M. E. Banks,
maria.e.banks@nasa.gov

Citation:
Banks, M. E., Fenton, L. K., Bridges, N. T., Geissler, P. E., Chojnacki, M., Runyon, K. D., et al. (2018). Patterns in mobility and modification of middle- and high-latitude southern hemisphere dunes on Mars. *Journal of Geophysical Research: Planets*, *123*, 3205–3219. https://doi.org/10.1029/2018JE005747

Received 2 JUL 2018
Accepted 30 OCT 2018
Accepted article online 8 NOV 2018
Published online 26 DEC 2018

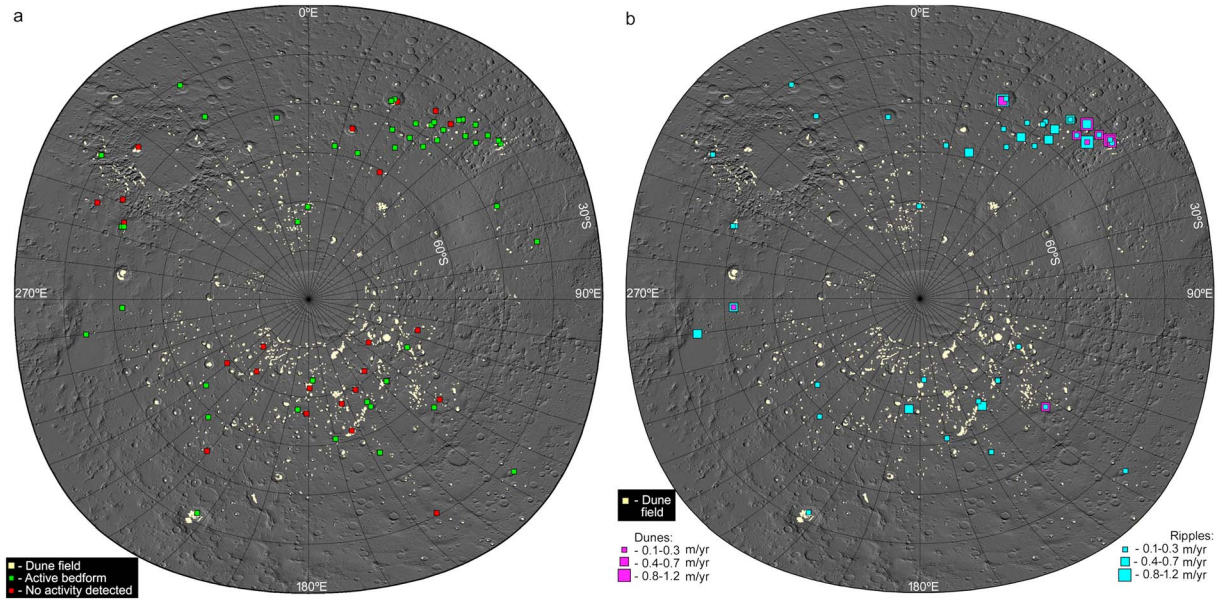

Figure 1. (a) Locations of dune fields and sand sheets (yellow; dune fields poleward of 50°S latitude are from Hayward et al. (2007a, 2012) and those equatorward of 50°S latitude are from Hayward et al. (2007a, 2007b) or provided by coauthor Fenton), and locations where HiRISE image pairs were used to assess bedform mobility (red and green squares). Transverse aeolian ridges (TARs) are not included. (b) Migration rates of dunes (magenta) and ripples (cyan). The maps were constructed using Java Mission-planning and Analysis for Remote Sensing (JMARS; Christensen et al., 2009) using Mars Orbiter Laser Altimeter (MOLA) shaded relief as a base map (Smith et al., 2001).

near-surface sediments, not cemented in the ground ice, continue to migrate as superposing ripples. Understanding the characteristics of the activity and morphology of dune fields can provide valuable insight into local and regional sedimentary and climatic histories on Mars and Earth. Our results may reflect more than one generation of dune building and possibly a current phase of episodic activity and may have implications for shifts in the climate to activate or stabilize dune fields and sand sheets over time.

1. Introduction

The multiple dune fields and sand sheets observed on Mars attest to the importance of wind-driven (aeolian) activity in shaping the Martian surface, at least in its more recent geologic history. Multiple studies have now revealed present-day movement of sand by the wind and migration of bedforms (dunes and ripples collectively) in some environments in the current Martian climate and ~6-mbar atmosphere (e.g., Banks et al., 2015; Banks et al., 2017; Bourke et al., 2008; Bridges et al., 2010, 2012, 2013; Chojnacki et al., 2011, 2014, 2015, 2017, 2018a, 2018b; Fenton, 2006; Silvestro et al., 2010, 2011, 2013, 2016; Sullivan et al., 2008). Dune field and sand sheet formation, activity, and stabilization, on both Earth and Mars, are driven by factors such as sediment availability and wind transport capacity, potentially initiated by changes in climatic conditions (e.g., Ayoub et al., 2014; Ewing et al., 2010; Fenton et al., 2015, 2018; Fenton & Hayward, 2010; Kocurek, 1998; Kocurek et al., 2007; Kocurek & Lancaster, 1999; Runyon, Bridges, Ayoub, et al., 2017; Silvestro et al., 2015). Bedforms that have become stabilized may be reactivated by an increase in the inflow of available sand; their morphology may evolve as a result of shifting wind regimes, or degrade (e.g., rounded dune brinks; dune morphologies that are difficult to discern) after extended periods of inactivity. Therefore, understanding the characteristics of the activity and morphology of dune fields can provide valuable insight into the local and regional sedimentary and climatic histories. Additionally, such analyses can add to our understanding of the interplay of aeolian and nonaeolian (e.g., periglacial, polar, volatile-driven) processes, the conditions associated with these processes, and potentially how they have changed over time.

Change detection analyses using repeat images (with scales as fine as 0.25 m/pixel) acquired by the High Resolution Imaging Science Experiment (HiRISE) onboard the Mars Reconnaissance Orbiter (McEwen et al., 2007) can now be used to assess aeolian bedforms for changes and migration over multiple Mars years (Figure 1). Prior work by Fenton and Hayward (2010) mapped and categorized dune fields into six

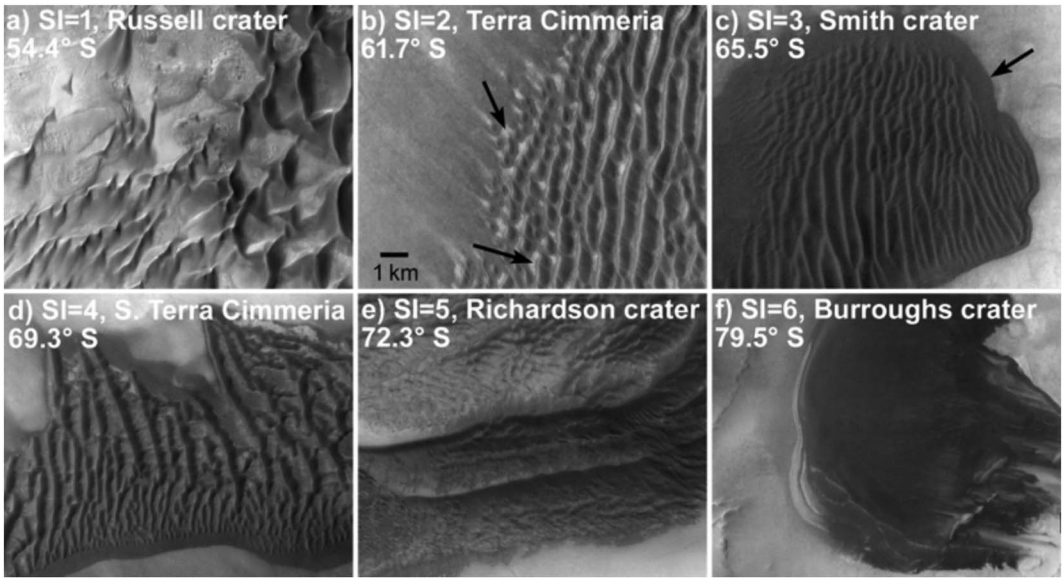

Figure 2. Type location dune fields exhibiting six morphological categories interpreted to correspond with a progression toward stabilization with stabilization indices (SI) ranging from 1 through 6 (see Table 1). (a) SI = 1: these dune fields are typical of most found at low latitudes on Mars. (b) SI = 2: a crisp-edged sand apron surrounds dunes and partially spans interdunes (arrows point to windows in apron). (c) SI = 3: the sand apron (black arrow) spans all interdunes and dune crests may be rounded. (d) SI = 4: dunes are harder to identify, and their surfaces are somewhat dissected. (e) SI = 5: dunes are increasingly dissected and difficult to identify. (f) SI = 6: dunes are not present, merely a sand sheet on a layered deposit. In all images, north is up. The scale bar is the same for all images.

morphological classes based on an inferred level of stability derived from the apparent presence/lack of superposed nonaeolian features and apparent degree of degradation by nonaeolian processes (see further description in section 2 and Figures 2 and 3); however, they were not able to corroborate their results with a change detection survey at that time. Fenton and Hayward (2010) identified a progressive southward trend toward nonaeolian modification, proposing that near-surface ground ice at high latitudes inhibits aeolian processes. Modeling work by Mellon et al. (2008) also demonstrated that ice tables can occur at ~2–6-cm depth in polar regoliths, likely including dune sand. Accordingly, we hypothesize that if ground ice is indeed a factor stabilizing the southern hemisphere dunes, then dune and ripple mobility, especially dune mobility, should decrease with an increasing prevalence of nonaeolian modification features at high-southern latitudes.

Using results from aeolian change detection and morphological analyses, we investigated aeolian bedform *mobility* (i.e., evidence of wind-driven migration or activity of bedforms and sediments and characteristics of that activity, such as migration rate) and *modification* (i.e., apparent presence/lack of superposed nonaeolian features and/or evidence of changes or degradation by nonaeolian processes) for 70 Martian dune fields and sand sheets located south of 40°S latitude (Table S1 and Figure 1). For this study we chose dune fields

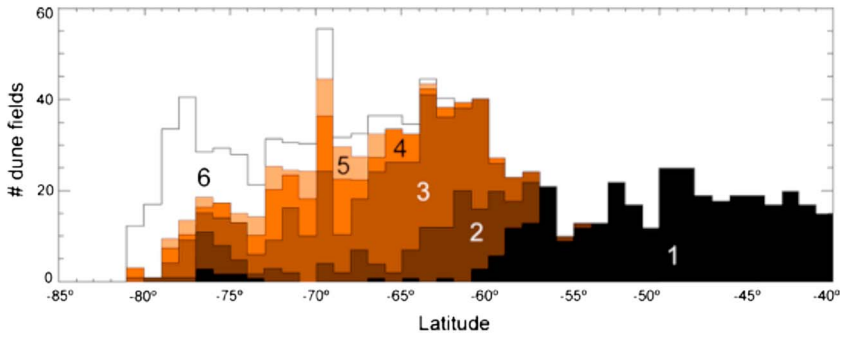

Figure 3. Latitudinal distribution of southern hemisphere dune fields by SI (Fenton & Hayward, 2010; Gullikson et al., 2018; see Tables 1 and S1).

Table 1
Morphological Dune Field Classes From Fenton and Hayward (2010) and Their Respective Stability Index (SI) Used in This Study

SI	Dune Field Class	Latitude	Characteristic Morphological Features[a]
1	Russell crater	<60°S	Identifiable dunes, crisp slip face brinks
2	Terra Cimmeria	57–66°S	Partial apron, slip face brinks may be rounded
3	Smith crater	58–79°S	Aprons span interdunes, slip face brinks often rounded
4	S. Terra Cimmeria	64–74°S	Aprons often span interdunes, slip face brinks often rounded, somewhat dissected surface
5	Richardson crater	65–79°S	Slip faces difficult to identify, dissected appearance
6	Burroughs crater	65–82°S	No dunes present

[a]See Figure 2.

with repeat HiRISE image coverage. For each location we (1) conducted change detection analysis with the HiRISE temporal image pairs, seeking evidence of wind-driven movement of sediments and migration of dunes and/or ripples superposing dunes or superposing sand aprons or sand sheets, and (2) applied a morphological stability index (SI) from the work of Fenton and Hayward (2010) and Gullikson et al. (2018) (see section 2 and Tables 1 and S1). A main objective of this study was to assess the relationship between the morphology and activity of dune fields and the relationship of these characteristics to their proximity to the south pole. A shift toward reduced bedform activity along with an increase in widespread dune degradation could be a likely result of cemented sediments, potentially by ground ice, consistent with the findings of Fenton and Hayward (2010). We also explored other possible factors (i.e., elevation and sand drift potentials derived from the NASA Ames Mars Global Climate Model (MGCM)) that may play a role in influencing the characteristics of the bedforms, and discuss implications for episodic phases of bedform reworking and potential correlations with climate-related activation or stabilization.

2. Background

The Mars Global Digital Dune database (MGD^3; Hayward et al., 2007a, 2007b, 2010, 2012, 2014) shows that large dark dunes are common both at northern-high latitudes (75% of mapped dune field coverage occurred from 70 to 90°N) and southern-high latitudes (15% of mapped dune field coverage occurred from 60 to 80°S; Figure 1). These circumpolar locations were noted in Viking-era global surveys (e.g., Thomas, 1982; Ward et al., 1985); in particular, Thomas (1982) speculated that high-latitude dunes in both hemispheres were sourced from nearby polar-layered terrain. However, the similarity between northern and southern dunes ends upon closer inspection. Whereas most bedforms in the northern hemisphere show aeolian-driven movement, particularly in the high-northern latitudes (>70°N), the same is not always the case in the southern-middle to southern-high latitudes (e.g., Bridges et al., 2013; Banks et al., 2015; Chojnacki et al., 2018a). Further, the dune fields of the southern-middle to southern-high latitudes exhibit a wide range of latitudinally varying morphological features that have no known counterpart in the northern hemisphere (e.g., the sand aprons and dissected surfaces mapped by Fenton and Hayward (2010) have not been reported in northern latitudes).

Looking at the latitude range from 50 to 90°S, previous work by Fenton and Hayward (2010) mapped and categorized dune fields into six morphological classes based on an inferred level of stability visible in Thermal Emission Imaging System (THEMIS) visible (VIS) (Christensen et al., 2004), Context Camera (CTX) (Malin et al., 2007), and Mars Orbiter Camera (MOC) (Malin et al., 1991) images (see Figure 2); this selection of images collectively offered suitable coverage of dune fields for feature identification and classification. As part of an update to the MGD^3, all other dune fields in the south polar and equatorial MGD^3 (spanning 90°S to 65°N) were later categorized into these six morphological classes (Gullikson et al., 2018) using the same methods as Fenton and Hayward (2010). This more recent work assigned each dune field a stability index (SI) integer (number 1 through 6) corresponding to each type location; higher SI values correspond to increasing prevalence of features and morphological characteristics interpreted to indicate increased stability and nonaeolian modification (see text below; Table 1 and Figure 2).

Morphological characteristics considered in the determination of SI in the studies of Fenton and Hayward (2010) and Gullikson et al. (2018) include (1) the presence or absence of sharply edged sand aprons surrounding dune margins and/or a diffuse-edged sand sheet adjacent to the dune field, (2) the crispness of dune

brinks, (3) the readiness of identification of dune types (e.g., barchan, star), (4) the presence or absence of layers underlying the dune field, (5) the presence or absence of relatively bright material apparently superimposed on the dunes, (6) a smooth or dissected appearance at scales >30 m, and (7) the presence or lack of discernible dunes (Table 1). Dune fields with SI = 1 are typical of most large dark dunes on Mars, with identifiable dune forms and, where present, crisp slip face brinks (Figure 2a); all dune fields between 40 and 55°S latitude fit into this category (Figure 3). Between ~55 and 65°S latitude, different features emerge, with dunes exhibiting rounded brinks and dune fields being surrounded either partially (SI = 2; Figure 2b) or completely (SI = 3; Figure 2c) by an abruptly edged sand apron. Fenton and Hayward (2010) interpreted the rounded brinks and aprons as indicators of nonaeolian (perhaps ice-related) erosional processes competing with aeolian dune construction (which is characterized by features such as crisp dune brinks), limiting the ability of the wind to rework bedforms. Poleward of ~65°S latitude, many dune fields take on an even further degraded appearance in which individual dunes are progressively more difficult to identify (SI = 4, 5; Figures 2d and 2e). Fenton and Hayward (2010) interpreted these morphological characteristics as evidence of progressive erosion by nonaeolian processes and progressive stabilization of the dune fields. The most poleward dune fields, found mainly between 70 and 82°S latitude, are simply dark sand sheets (SI = 6; Figure 2f); these were proposed to be either fully eroded dune fields or locations where dunes were unable to form.

Fenton and Hayward (2010) observed that the shift in dune morphology poleward of ~60°S latitude (where SI = 2 dune fields first appear) corresponded with concentrations > ~20% of near-surface water equivalent hydrogen in Mars Odyssey Neutron Spectrometer maps; these concentrations are interpreted to be ground ice (Feldman et al., 2004; Wilson et al., 2018). In addition, two-layer thermal modeling of the near-surface properties of southern hemisphere dune fields using Thermal Emission Spectrometer (TES) and THEMIS data also suggested that that dune fields with SI = 1 and 2 are distinct from those with SI ≥ 3 (Hoover et al., 2018). Fenton and Hayward (2010) proposed that ground ice acts as a dune-stabilizing agent, inhibiting aeolian sand transport that would otherwise rework dunes and ripples (see further discussion in section 4.5). Similar processes seem to operate in terrestrial polar dune fields; Bourke et al. (2009) demonstrated that dune migration in Antarctica may be slowed by the presence of niveo-aeolian deposits.

3. Methods

3.1. Dune Fields

We chose 70 dune fields in our study area (40°–90°S latitude) that are covered by HiRISE temporal image pairs (Figure 1). For dune fields not already included in the MGD[3], dune morphological types were classified following a similar approach (Hayward et al., 2007a, 2007b) and include sand sheets, barchan, barchanoid, transverse, linear, and star dunes as defined by McKee (1979). Bedform classes in our analysis include large dunes, and meter-scale ripples superposing dunes or superposing surrounding sand patches, aprons, and sand sheets (Table S1). We did not include transverse aeolian ridges (TARs) in our analysis as these are commonly found to be inactive regardless of latitude (e.g., Bridges et al., 2012; Zimbelman, 2000).

3.2. BedForm Mobility

For each of the 70 dune fields, change detection analyses were conducted with HiRISE temporal image pairs for evidence of activity, and compared to each dune field's SI (Figure 1 and Table S1). Images selected for the change detection analyses were separated in time by one or more Martian years (typically two to four Mars years) and were filtered to include only those acquired under similar conditions including: camera roll angles (within ~10°), illumination geometries such as solar elevation angle (acquired at the same time of the year and near the summer solstices), and solar azimuth (constrained to within ~10°; Bridges et al., 2012, 2013). Map-projected images were overlaid and coregistered to immobile tie points (i.e., permanent surface features, fractures, large rocks) and analyzed in ArcGIS for detection of changes in the bedforms over time. Bedforms were investigated for movement in multiple locations throughout each HiRISE image. Movement or migration was quantified by measuring bedform displacement; for example, in the case of ripples, the distance between the margins of ripple crests and the nearest tie points was measured in each image in the pair and then differenced. Where possible, displacement was measured for at least 10 bedforms and averaged. We completed displacement measurements on relatively flat surfaces, at roughly the same elevation as the surrounding surface and tie points, to minimize error from topography (e.g., dune displacements measured at the base of dune slip faces, ripple displacements measured on the flatter surfaces along the

edges of dunes or on the extended horn of a barchan). We estimate an error of ~1–2 pixels (±25–50 cm) for displacement measurements. Where substantially differing displacements were observed within the same HiRISE image or dune field, they were recorded as separate data points at the same location. Migration rates were determined using the time interval between acquisition of each image and were reported in units of meters per Earth year (m/yr). For sand sheets or aprons lacking dunes or ripples, changes in margins were also reported if detected. We evaluated dunes and ripples separately for evidence of changes and migration; data for dunes and ripples are differentiated in Table S1, as are data for ripples superposing dunes and ripples superposing sand sheets, sand aprons, or sand patches.

3.3. Atmospheric Modeling

Atmospheric models have long been used to provide context for sand-transporting winds on Mars (e.g., Armstrong & Leovy, 2005; Fenton & Richardson, 2001; Greeley et al., 1993). Global climate models calculate the state of the atmosphere as a set of points that forms a three-dimensional grid around the surface of Mars, outputting atmospheric and surface parameters at each grid cell (e.g., wind velocity, air temperature, air pressure). Global-scale circulations simulated by global climate models broadly agree with the observed alignment of aeolian features, such as wind streak orientations (e.g., Fenton & Richardson, 2001; Greeley et al., 1993). However, spatial patterns of wind stress are strongly influenced by small-scale topographic features that global climate models often do not resolve (e.g., Toigo et al., 2012). Despite such known inaccuracies, it is plausible that large-scale flows, such as that driven by Hadley circulation and thermal tides, could enhance sand-transporting winds at some latitudes more than at others. If this is the case, then the general circulation could explain the observed poleward trend toward dune stability, rather than stabilization by ground ice. In this work we test whether such a latitudinal trend in wind stress exists. The NASA Ames Mars Global Climate Model (MGCM) has been used extensively to investigate Mars' climate (e.g., Haberle et al., 1999; Kahre et al., 2006). The model numerically calculates the state of the atmosphere as a set of points that forms a three-dimensional grid around the surface of Mars, outputting atmospheric and surface parameters at each grid cell (e.g., wind velocity, air temperature, air pressure).

For work involving the MGCM (section 3.3), we simulated one Mars year with a grid spacing of 5° of latitude by 6° of longitude and a temporal resolution of 1.5 hr (in which an *hour* is 3698.7 s long or 1/24th of a Martian sol). Winds produced by features at scales smaller than the resolution of the MGCM grid (e.g., local topographic relief) cannot be represented by the MGCM. Rather, the modeled atmospheric conditions are dictated by regional- and global-scale weather patterns (e.g., baroclinic waves) and surface features (e.g., $>$ ~200-km baseline topographic relief). We estimated a sand drift potential at each time step and (surface) grid cell, assuming that all dune sand consists of 100-μm basalt grains, by determining local time-dependent threshold friction velocities to estimate potential sand fluxes using the relation from Kok (2010) (note that Kok (2010) assumes that the grain density is 3,000 kg/m^3, which is appropriate for basalt grains). Summed over a Mars year, these values provide an estimate of the net *windiness* at each grid cell.

4. Results and Discussion

4.1. Spatial Distribution of BedForm Mobility

Out of the 70 locations examined in our study area, 49 of these locations, or roughly 70% of the dune fields, showed evidence of wind-driven movement or bedform migration. The other 21 locations did not reveal evidence of migration or activity (Figure 1 and Table S1). A lack of visible evidence of migration or activity indicates that either (1) there has been a temporal bedform-stabilizing change in the environmental conditions that previously enabled formation of the bedforms (such as a change in the available sediment supply; Ewing & Kocurek, 2010) or (2) the bedforms are moving at a rate below the HiRISE detection limit for the time interval between repeat image acquisition combined with the resolution of the images (i.e., the bedforms have migrated a distance that is less than ~3 pixels, which in most cases is less than ~75 cm, over the baseline; see Table S1; Bridges et al., 2013). In all dune fields where dunes are observed to migrate, ripples were also observed to migrate. However, not all dunes were observed to migrate in dune fields with migrating ripples.

Migration rates in our study area range from ~0.1 to 1.2 m/yr with an average of 0.4 m/yr for dunes and ~0.3–0.4 m/yr for ripples. These results are below the average migration rate of ~0.7 m/yr estimated from global studies of dunes on Mars (Banks et al., 2014; Bridges et al., 2013). For 10 dune fields, bedforms (either

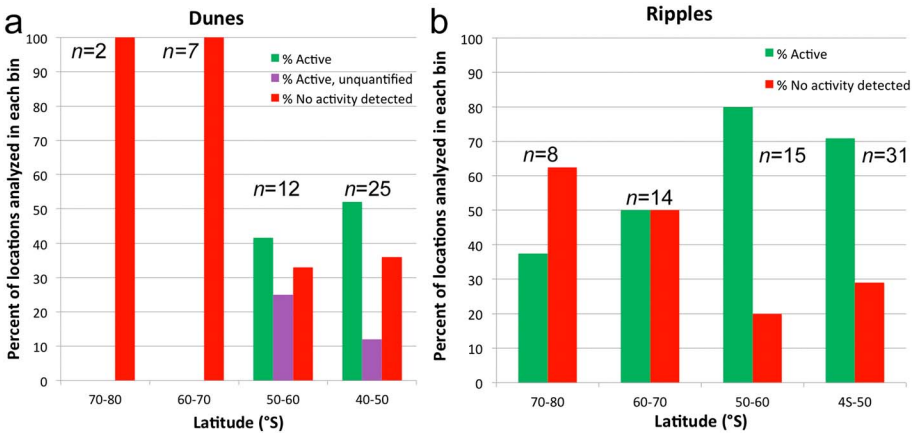

Figure 4. Percentage of (a) dunes and (b) ripples showing activity (green) or no evidence of activity (red) by latitude. Note the shift in prevalence of active ripples, and the lack of active dunes south of ~60°S latitude. In (a), dunes with ambiguous changes or difficult to measure movement are classified as *active, unquantified* (purple). These dunes are observed more frequently closer to 60°S latitude; they potentially show an increasing stabilization of the dunes, especially relative to the ripples, with increasing latitude.

dunes or ripples, but typically dunes) showed evidence of activity or migration, but the changes were ambiguous and difficult to reliably measure. Examples belonging to this category include small ripples at the limit of detection that were moving but could not be sufficiently resolved for measurements, dunes undergoing deflation, or shifting of sediments at the edges of dune fields and surrounding sand patches. In these instances, the bedforms were cataloged as mobile or active, but do not have a migration rate (classified as *active, unquantified* in Table S1).

There is a general decrease in evidence of activity with increasing latitude (Figures 1, 4, and 5). Only ~22% of the sites between 40 and 60°S latitude appear to be inactive, but that percentage increases to ~55% of the sites south of 60°S, and >60% of the sites south of 70°S (Figures 1 and 4). The most poleward measurement of dune activity was observed at ~57°S latitude; no dunes at latitudes south of this latitude exhibit migration. Ripples are also increasingly inactive with increasing latitude, although some active ripples were observed well into the high-southern latitudes and as far south as ~74°S (Figures 1, 4, and 5). At six locations, ripples superposed on dunes were observed to migrate, while the dunes themselves either did not show evidence of movement, or the movement was so subtle and ambiguous that it could not be quantified (Table S1 and Figure 4). These observations were more common at latitudes within ~10° of 60°S and may reflect the increasing stabilization of bedforms with increasing latitude.

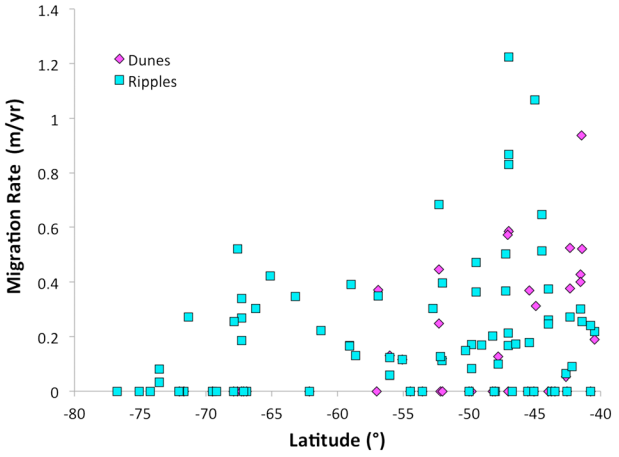

Figure 5. Average migration rates for dunes (magenta) and ripples (cyan) plotted by latitude. Bedforms that show no evidence of activity (inactive) and active bedforms with ambiguous or unquantified movement plot with a migration rate of 0.

Results show a broad distribution of ripple migration rates (~0.1–1.2 m/yr) with ripples migrating at or below the average rate for the study area (~<0.4 m/yr) at a wide range of latitudes (Figures 1b and 5). Ripples may exhibit a slight decrease in average migration rate poleward, although this may be more indicative of regional variation in activity. The highest migration rates for both dunes and ripples in our study area (>0.8 m/yr) were observed in Noachis Terra, particularly in Hellespontus Montes (up to ~1.1 m/yr) and within Kaiser crater (up to ~1.2 m/yr). Migration rates at similar latitudes but other longitudes are closer to the global average (e.g., in Icaria Planum and northwest Aonia Terra; ~0.6–0.7 m/yr). The localized occurrence of our fastest migrating bedforms within such close geographical proximity, particularly within Noachis Terra, may be related more to regional trends in wind strength than to a larger-scale latitudinal shift in stabilization factors. For example, Chojnacki et al. (2018a) also found some of the highest Martian sand flux rates for bedforms in the Hellespontus Montes region. They attributed the high rates to the proximity of the dunes to Hellas Basin, serving as a strong topographic gradient, and likely associated anabatic slope winds.

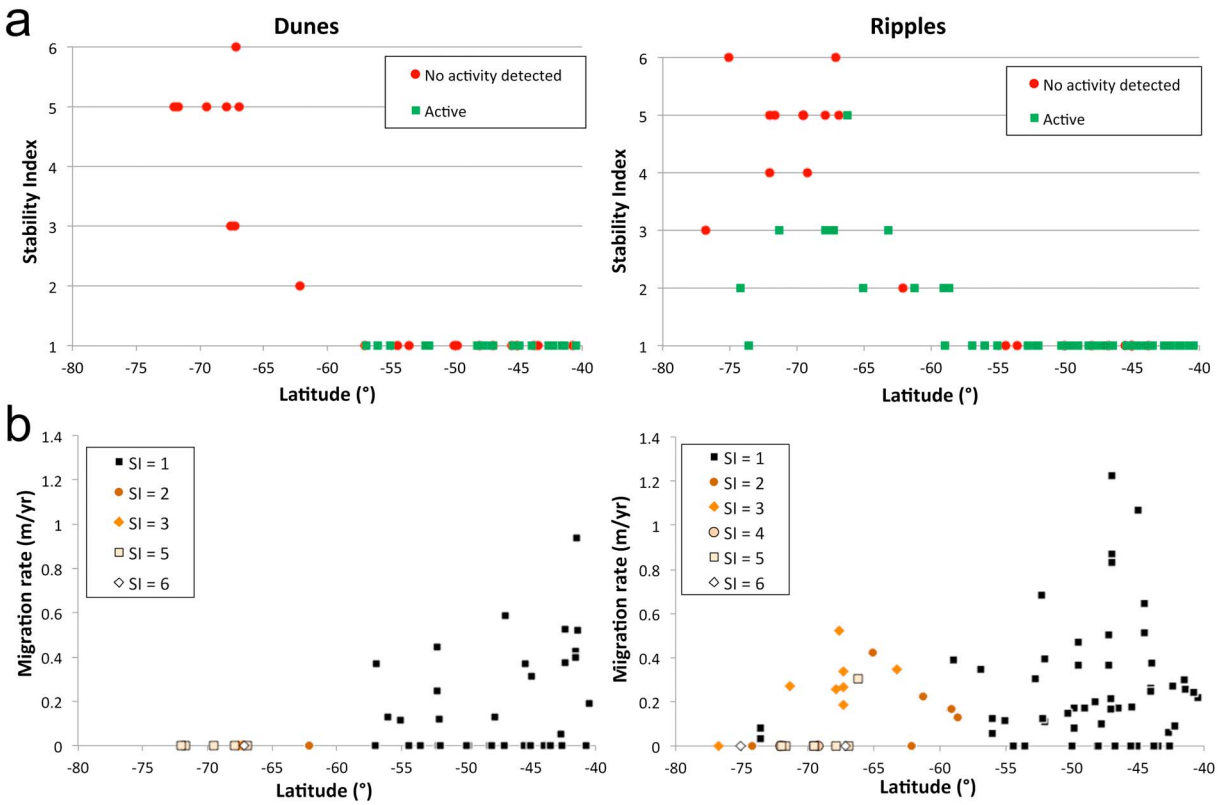

Figure 6. (a) Dune field stability index with latitude, marked by (left) dune and (right) ripple mobility. Note the near lack of mobility for ripples in SI ≥ 4 dune fields and for dunes in SI ≥ 2 dune fields. (b) Average (left) dune and (right) ripple migration rates with latitude, colored by dune field stability index. Bedforms that show no evidence of activity (inactive) and active bedforms with ambiguous or unquantified movement plot with a migration rate of 0. Note the decrease in migration rates with higher SI.

4.2. BedForm Mobility and Apparent Stability Index

Figure 6 shows dune and ripple mobility in relation to latitude and SI. As discussed in section 2, all dune fields north of ~55°S latitude have an SI of 1 (see Figure 3). With only a few exceptions, all measured bedforms in SI = 1 dune fields are active (Table S1 and Figure 6a). All measured dunes south of 60°S are both inactive and have SI values >1. Nearly all active ripples found south of 60°S are located in dune fields with no to moderate morphological signs of stability, or SI = 1–3 (see Table 1). With only one exception, bedforms in dune fields (dunes and ripples) and sand sheets (ripples) with SI ≥ 4 (a total of 10 unique locations in this study) are inactive and show no evidence of movement (see Table 1 and Table S1 and Figure 6a). Figure 6b shows how dune and ripple migration rates vary with latitude and SI. As was already discussed, the fastest ripples and dunes are all located equatorward of 60°S and here we see that these faster migration rates are also all observed in SI = 1 dune fields. The lack of higher migration rates (>0.4 m/yr) at high latitudes (>~60°S) and in dune fields with SI > 1 is consistent with the interpretation that dune fields with greater SI are more stabilized.

It should be noted that dunes and ripples that appear to be inactive based on change detection analyses are not necessarily being degraded, such as the SI = 1 dune fields shown in Figure 6a that exhibit no evidence of activity. A reduced level or apparent lack of present-day aeolian activity may simply indicate a change in the conditions that originally made formation and migration of the bedforms possible, such as favorable wind strength and ample sediment supply and availability. For the dune fields located north of ~55°S latitude, conditions appear to have remained favorable for aeolian activity at present, or until relatively recently. On the other hand, the SI > 1 dune fields located south of ~55–60°S latitude provide evidence of a process degrading the bedforms that is dominant over or acting at a faster rate than aeolian processes at these higher latitudes. A greater prevalence of degradation, or higher SI values, also likely corresponds with an increased duration of bedform inactivity (Fenton & Hayward, 2010).

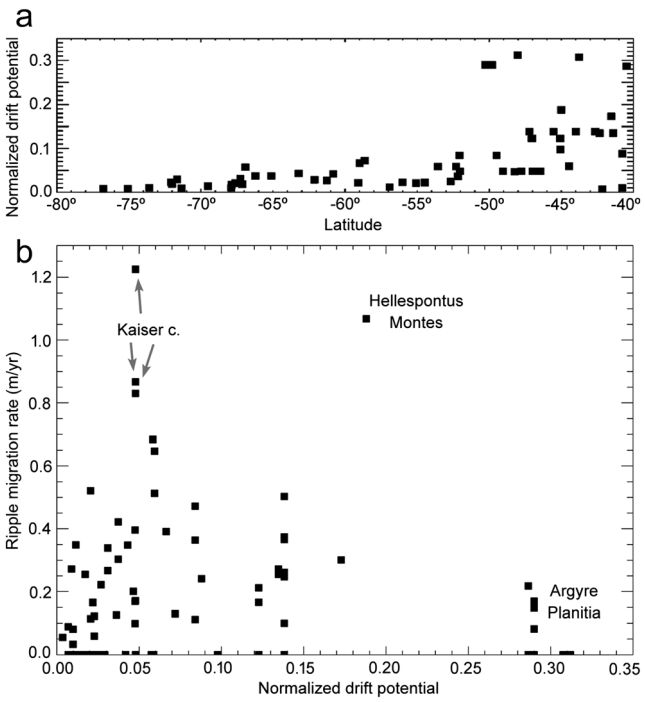

Figure 7. (a) MGCM-derived annual drift potential (normalized to the global maximum) for model grid cell locations corresponding with ripple measurements. (b) Normalized annual drift potential versus average ripple migration rates from Table S1. Measured ripple migration rates do not correlate with MGCM-derived drift potential, likely as a result of strong mesoscale flows that are not well resolved at the MGCM scale.

4.3. BedForm Mobility, Apparent Stability, and Annual Drift Potential

Annual drift potentials derived from the Ames MGCM were normalized to the global maximum annual drift potential. Figure 7a shows the latitudinal distribution of normalized drift potentials pulled from model grid cells corresponding to locations of ripple measurements. As was shown in section 3.2 and Figure 6b, results show a lack of high migration rates at high latitudes and in dune fields with higher SI values (SI $>$ 1) pointing to processes that are acting to stabilize the bedforms. However, MGCM drift potentials also decrease toward the pole, suggesting that bedform migration rates may be inhibited by the relative weakness of impinging winds as much as by other factors. The drift potentials span the entire Martian year, without removing periods of CO_2 frost cover that could retard ripple and dune migration; including this effect would further suppress high-latitude drift potentials.

The plots in Figures 6b and 7a suggest that there may be a correlation between ripple migration rate and MGCM-derived drift potential. However, Figure 7b shows that this relationship is not so straightforward ($r = -0.03$, $p < 0.79$). The highest drift potentials correspond with strong winds on the western rim of Argyre Planitia, whereas the highest measured ripple migration rates occur in Noachis terra: in Kaiser crater and Hellespontus Montes. The lack of agreement between the two results is probably one of scale. Meter-scale ripples may be influenced by the regional- and global-scale wind patterns that are well represented by the MGCM, but in many locations their activity may be controlled by locally enhanced winds that the MGCM cannot resolve. Further study with mesoscale models could provide a better match with measured bedform migration rates; disparities between mesoscale drift potentials and migration rates could potentially be attributed to stabilization processes (e.g., ground ice).

4.4. BedForm Mobility, Apparent Stability, and Elevation

All but three locations analyzed in this study occur at elevations between ~ −3,000 m below and 2,000 m above the datum for a total elevation range of only ~5 km for the vast majority of the bedforms in our data set. One of the outliers is located at an elevation of ~ −4,000 km and exhibited no evidence of activity; the other two outliers are located at ~ −7,000-km elevation and were classified as active but movement could not be quantified (see Table S1). Figure 8a shows that there is no clear trend in the mobility of the bedforms in relation to elevation; we generally see both active and inactive bedforms throughout the range of elevations. We also considered the variation in SI combined with mobility in relation to elevation (Figure 8b). All dune fields with SI $>$ 1 occur within the top 1.5 km of the elevation range of the dune fields in our study area. However, these dune fields with SI $>$ 1 are also located at higher latitudes (>60°S; see Figure 8a), suggesting that the corresponding increase in SI is likely to be a function of latitude, rather than elevation.

Globally, Mars has an elevation range of nearly 30 km. Nearly all bedforms in the low-lying north polar sand seas that have been analyzed for activity have been found to be mobile (e.g., Banks et al., 2015; Bridges et al., 2013; Middlebrook, 2015). In contrast, bedforms at the very highest elevations, on a global scale, appear to be immobile (e.g., Banks et al., 2015; Bridges et al., 2013), leading to the question of whether or not bedforms are more active at lower elevations. Given that the friction velocity for sand saltation u^* is related to the air density ρ_{air} and shear stress τ such that $u^* = \sqrt{\frac{\tau}{\rho}}$ (e.g., Shao & Lu, 2000), it is reasonable to infer that winds are more likely to exceed the saltation threshold at lower elevations with higher atmospheric density (e.g., Armstrong & Leovy, 2005), and that therefore bedforms in these locations would more likely be mobile. If Mars experienced the same wind speeds at all locations at the same time, then this would certainly be the case. For example, at −3,000- and 2,000-m elevations, we estimate that the surface air pressure would seasonally range between 6.4–8.4 and 4.5–5.3 mbar, respectively (Withers, 2012). These differences in pressure have an appreciable effect on threshold friction speed. For example, the fluid threshold friction speed for ~120-μm sand at 5 mbar is u^* = ~1.9 m/s, whereas at 10 mbar the threshold is 45% lower at u^* = ~1.3 m/s (Greeley and Iverson,

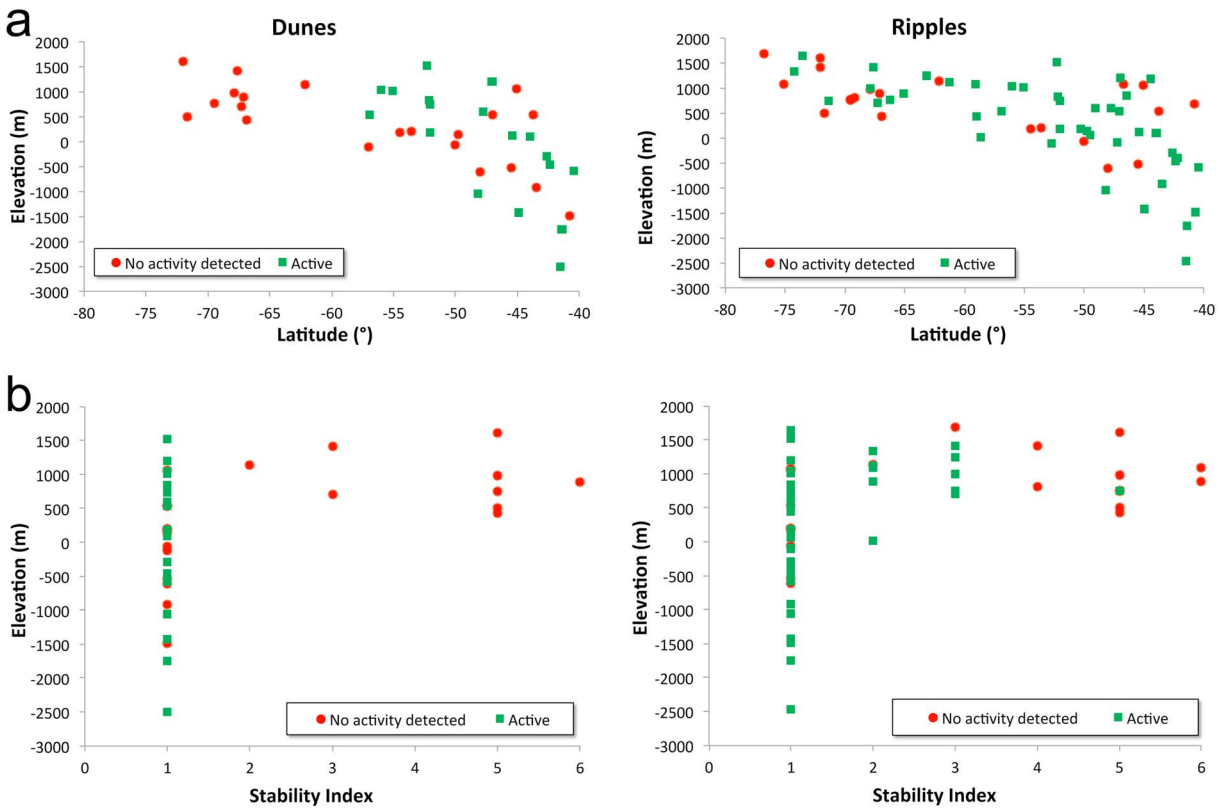

Figure 8. (a) Mobility of (left) dunes and (right) ripples with elevation. (b) Mobility and SI at different elevations for (left) dunes and (right) ripples. Elevation is in meters above and below the datum. Note that three outliers at very low elevations have been omitted from these plots to focus on the majority of the bedforms which occur within this elevation range (see text in section 4.4). There is a slight overall increase of elevation with latitude. We generally see both active and inactive bedforms throughout this entire elevation range. Dune fields with higher SIs consistently occur only within the upper half of the elevation range (at elevations ~500 m and higher). However, the higher elevations in our study area also correspond with higher latitudes (a), such that polar processes may potentially play a larger role in influencing dune modification processes than elevation.

1985). However, winds on Mars are not uniform in space and time. Considering bedform mobility globally, a potential influence of elevation and associated atmospheric pressure on observed bedform activity is so far only apparent at the extreme highest and lowest elevations of Mars (Banks et al., 2015), neither of which are represented in the elevation range of the dune fields included in this study (primarily between −3,000 and 2,000 m). Thus, while variations in elevation, and associated atmospheric pressures, may potentially play a small influential role in enhancing or inhibiting the mobility of bedforms or the prevalence of nonaeolian processes, our results do not indicate that this is a significant contributing factor in our studied dune fields.

4.5. Polar Processes

Results indicate a significant shift in both dune field activity and morphologic characteristics at ~60°S latitude. At roughly this latitude, the first dune fields with SI $>$ 1 appear; south of this latitude, ripples show decreasing mobility and dunes cease to be active at all (Figures 4–6 and Table S1). Most dune fields south of 60°S also exhibit morphologic characteristics that transition from familiar and identifiable dune types with sharp dune brinks to degraded features and increasingly unrecognizable dune types (Fenton & Hayward, 2010). Additionally, as previously discussed, neutron data from the Neutron Spectrometer show a shift at ~60°S latitude in the water-equivalent hydrogen content of the Martian regolith (Feldman et al., 2004; Wilson et al., 2018), which is interpreted to indicate an increase in ground ice. In accordance with Fenton and Hayward (2010), we propose that our observations of decreasing bedform mobility support the accumulation of ground ice between dune sand grains which may be stabilizing the grains and reducing sand availability in present climate conditions. As such, this accumulating ground ice would inhibit aeolian sand transport that would otherwise rework dunes and ripples eliminating or preventing development of erosional features (e.g., rounded dune brinks; e.g., Bourke et al., 2009). Additionally, dust infiltration between ice-cemented sand

grains could further immobilize bedforms (Bridges et al., 2010), and possibly enable cementation and recrystallization processes to operate and lithify dunes and sand sheets (Runyon, Bridges, Newman, et al., 2017).

Ground ice properties at Mars Phoenix Lander's landing site (68.22°N) are likely representative of ice-rich permafrosts elsewhere on Mars (Mellon et al., 2009). This is evidenced by crater-exposed ice in other locations on Mars, estimated to be of similar concentrations to those observed at the Phoenix landing site (Byrne et al., 2009). At the Phoenix landing site, ice table depths were observed at an average depth of 4.6 cm with variations up to 10 times this depth (Mellon et al., 2009). Importantly, the Phoenix lander explored its region during the northern summer when ice would be most scarce, thereby placing minimum constraints on the amount of cementing ice present. Mellon et al. (2009) demonstrated that ground ice on Mars can form from atmospheric water vapor diffusing into and freezing within existing pore spaces. Given the porous nature of dune sand and common dune heights of meters to tens of meters, most of a dune's interior could be immobilized by ice through this process. Thus, even in the Martian summer (Mellon et al., 2009), dunes at similar latitudes as that of the Phoenix landing site (both north and south) could have an icy core just beneath the surface. Observations at Phoenix's landing site also showed that exposed ice sublimed away within a few sols; as such, recently sublimed ice from a dune could then *release* sand grains to seasonally or episodically participate in aeolian motion.

Dunes in the large northern-high-latitude sand sea, Olympia Undae, are also interpreted to contain ice-rich cores (Feldman et al., 2008). However, in contrast, present-day aeolian-driven movement has been observed (e.g., Banks et al., 2015; Bridges et al., 2012, 2013; Hansen et al., 2011) and high sand fluxes have been estimated for these north polar dunes (Chojnacki et al., 2018a; Diniega et al., 2017). Their activity has been attributed to strong katabatic and anabatic winds associated with the nearby high-elevation polar cap (Ewing et al., 2010; Hayward et al., 2014; Horgan & Bell, 2012; Howard, 2000; Tanaka et al., 2008) compounded by the presence of seasonal volatiles (Bridges et al., 2013; Ewing et al., 2010; Hansen et al., 2011). There may be no analogous driver of strong winds near most high-southern-latitude dune fields, so that near-surface volatiles can more effectively lock dunes in place. Elevation may also play a small contributing role as the northern polar regions (outside of the north polar layered deposits) are generally much lower in elevation than the southern polar regions (see section 4.4). In addition, due to Mars' elliptical orbit and axial obliquity, the southern latitudes experience longer and colder winters than in the northern hemisphere, and stabilizing agents such as ground ice, dust, and salts (Bridges et al., 2010; Runyon, Bridges, & Newman, 2017) have longer periods over which to accumulate than they do in Olympia Undae in the north (Fenton & Hayward, 2010).

The longer and colder winters in the middle- to high-southern latitudes also result in significant water and CO_2 annual surface frost (e.g., Bridges et al., 2010; Dundas et al., 2012; Runyon, Bridges, & Newman, 2017) that covers the surface to seasonally stabilize bedforms for longer durations than elsewhere on Mars. Thus, over the course of a Mars year, even active bedforms in the middle- to high-southern latitudes have shorter frost-free periods of time during which migration is possible compared to other Martian bedforms. Our estimates of migration rates are averaged over durations of years. Thus, some bedforms in our study area may be migrating at similar rates to those in other locations on Mars, but are only able to migrate over a shorter period of time resulting in lower average migration rates over a yearly time span (~0.3–04 m/yr averaged over our study area) compared to the global average (~0.7 m/yr; Banks et al., 2014; Bridges et al., 2013). There is also a significant exchange of volatiles seasonally when CO_2, followed by trapped H_2O, sublimates as spring temperatures increase (e.g., Piqueux et al., 2008). Initial sand mobilization may not be a purely aeolian process: eruption of geysers (producing *spiders*) may create localized pockets of higher pressure and may loft sand grains allowing otherwise below-threshold winds to mobilize the sand downwind (Hansen et al., 2010; Portyankina et al., 2017). Similar processes are invoked for grain initiation on Pluto in which sublimation by nitrogen and other ices may initially loft grains, allowing Pluto's extremely sparse atmosphere to then saltate grains as part of proposed dunes (Telfer et al., 2018). Dunes and ripples located near the ~60°S latitude transitional zone may be particularly susceptible to intermittent activity due to seasonal ices.

For six dune fields in our southern hemisphere study area, ripples superposed on dunes are observed to migrate while the dunes themselves either are not moving, or are moving at a rate below the threshold of detection (i.e., less than ~3 HiRISE pixels during the observed baseline; Table S1 and Figure 4). All six of these dune fields are located between ~47 and 67°S latitude and all have an SI value of either 1 (those further north) or 3 (those further south). In some cases this observation could indicate a recent shift in

wind patterns, or the dunes may simply be moving at a much slower rate relative to the ripples; as smaller bedforms often migrate at faster rates compared to larger bedforms, the later might be expected in the absence of any additional stabilizing (i.e., ice-related) processes. However, we propose that these observations may reflect the spatial transition from the dominance of aeolian to nonaeolian processes (e.g., polar/periglacial processes), and a poleward latitudinal transition to further stabilization of the dunes from increasing amounts of ground ice, or from ground ice becoming increasingly stable closer to the surface. For example, some of these dune fields, presumably still located where sediment availability and wind conditions favor bedform migration, may have dunes stabilized by ground ice at their core while surface/near-surface sediments not cemented in the ground ice continue to move (i.e., saltation, reptation, creep) as superposing migrating ripples (Feldman et al., 2008; Fenton & Hayward, 2010).

Fenton and Hayward (2010) identified a juxtaposition within some high-latitude dune fields of relatively fresh-appearing dunes (i.e., with crisp slip-face brinks) occurring near those that are more degraded-appearing, and suggested that these dune fields may have experienced episodic reworking over time. Likewise, we find dune fields with co-located stabilized dunes and migrating ripples, and numerous dune fields with SI values as high as 3 that exhibit migrating ripples. Potentially, we are observing the coexistence of two depositional environments with competing dynamics of aeolian and ice processes strongly governed by local and regional boundary conditions. These boundary conditions can change over time and create shifting cryospheric and aeolian environments (e.g., Brothers & Kocurek, 2018). Additionally, we are potentially observing more than one generation of bedform construction and/or possibly we are in a current phase of reworking (Fenton & Hayward, 2010; Runyon, Bridges, & Newman, 2017). Since we can assume that these dune fields originally accumulated in an environment in which sand availability and wind transport capacity allowed sand saltation and dune accumulation, we can also interpret, in accordance with Fenton and Hayward (2010), the morphological shift to SI values >1 as a potential indicator of climate change post-dating the formation of the dune fields. As near-surface ground ice is thought to stabilize dunes and reduce sediment availability (e.g., Bourke et al., 2009), we would expect climatic changes that overprint local boundary conditions and influence the amount of near-surface ground ice to likely alter levels of dune activity. Thus, our combined observations of high-latitude dune mobility and modification may reflect a recent shift in the climate to activate or stabilize these dune fields. For example, studies have turned to variations in orbital parameters of Mars to explain climate change; Martian obliquity, which varies with a periodicity of 10^4–10^5 years and which can strongly influence insolation and change atmospheric density and wind strengths (Brothers & Kocurek, 2018; Haberle et al., 2003; Head et al., 2003; Laskar et al., 2004), likely serves as a cyclical climate forcing agent influencing the formation and stabilization of dune fields and sand sheets (e.g., Ayoub et al., 2014; Brothers & Kocurek, 2018; Fenton et al., 2018; Laskar et al., 2004; Runyon, Bridges, & Newman, 2017).

5. Conclusions

We investigated aeolian dune and ripple *mobility* and *modification* (stability index, or SI, of 1–6) for 70 dune fields and sand sheets poleward of 40°S latitude on Mars. For each dune field (dunes and ripples superposing dunes) and sand sheet (superposing ripples), we conducted change detection analyses with HiRISE temporal image pairs for evidence of activity, and compared results with each dune field's SI (Figure 1 and Table S1).

- Results show a decrease in sand mobility with increasing latitude and SI.
- Both dunes and ripples are more likely to be mobile at lower latitudes, although some high-latitude ripples are actively migrating.
- Dune fields with SI ≤ 3 are dominantly active while those with higher SIs are dominantly inactive (Figure 6).
- Migration rates range from ~0.1 to 1.2 m/yr with averages for both dunes and ripples of ~0.3–0.4 m/yr. This result is below the estimated average migration rate from global studies (~0.7 m/yr; Banks et al., 2014; Bridges et al., 2013). Ripples migrating at or below the average rate for our study area (~ $<$0.4 m/yr) are observed at a wide range of latitudes. Results suggest a slight overall slowing of bedform migration rates with increasing latitude and SI, although this might be a result of regional variation in activity. Additionally, annual average migration rates may be lower than global averages due to long and cold winters and thus shorter frost-free time spans during which migration of active bedforms is possible in the middle- to high-southern latitudes.

- In the northern part of our study area (~40°–55°S latitude), dune fields are mobile and are not degrading (SI = 1). Generally speaking, conditions where these dune fields formed, such as ample sediment supply and winds at or above saltation strength, remain favorable for aeolian activity today.
- In the high-southern latitudes (> ~60°S), it appears that conditions favorable to dune field and sand sheet activity have shifted to less favorable conditions in most locations, perhaps episodically, since the time of sand accumulation and dune formation.
- There is an apparent correlation between ripple migration rates and MGCM-derived drift potential, although in several locations, ripple activity appears to be controlled by locally enhanced winds not resolved by the MGCM (i.e., Noachis Terra and Hellespontus Montes regions).
- While the slightly higher elevations and associated lower air pressures at high-southern latitudes may play a small influential role, they do not appear to be a significant factor inhibiting the mobility of dune fields.
- The change in prevalence of active bedforms to those that are inactive as well as the shift in dune morphology toward characteristics consistent with stability and increasing nonaeolian modification (SI $\geq$ 2) both occur at ~60°S and coincide with the edge of high concentrations of H_2O-equivalent hydrogen content observed by the Neutron Spectrometer (Feldman et al., 2004; Wilson et al., 2018).
- Observations of decreasing bedform mobility with increasing latitude support the accumulation of ground ice between dune sand grains which may be stabilizing the grains and reducing sand availability in present climate conditions. Some dunes may be stabilized by ground ice at their core while surface/near-surface sediments not cemented in the ground ice continue to migrate as superposing ripples (Feldman et al., 2008; Fenton & Hayward, 2010).
- Dune fields with co-located inactive dunes and migrating ripples, and dune fields with SI > 3 that exhibit migrating ripples, may reflect more than one generation of dune building and/or a current phase of episodic reworking, and may have implications for shifts in the climate to activate or stabilize dune fields and sand sheets.
- Results indicate a link between mobility and SI, suggesting that in some cases we can potentially infer whether dunes are active, and some characteristics of that activity, based on their morphologic appearance.

As more high-southern-latitude temporal image pairs become available with repeat coverage of dune fields at time spans of less than a year (within a spring or summer season), further change detection analyses can answer questions about migration rates of dunes and ripples over shorter time scales in a polar environment. Further, such additional data will help reveal the influence of seasonal ice coverage and seasonal thawing on aeolian-driven movement and rates of movement. MGCM results combined with mesoscale models for orographic effects could take into account local topography and other factors that could increase or decrease potential sand drift. Further insight regarding the results presented here can also be provided through future polar volatile modeling and sand-ice wind tunnel studies.

Acknowledgments
We are grateful for the efforts of the many people responsible for the success of the MRO mission, particularly those at HiROC. Data are available from the NASA Planetary Data System (https://pds.nasa.gov/). Results are included in Table S1 in the supporting information. This manuscript benefitted from very helpful reviews from M. R. Balme, L. D. V. Neakrase, and M. Golombek. This research was supported by the NASA Mars Data Analysis Program (MDAP), grant NNX14AO96G. M. Chojnacki was supported by MDAP grant NNH14ZDA001N. K.D. Runyon was supported by MDAP grant NNX16AJ43G/123117. J.R. Zimbelman was supported by MDAP grant NNX12AJ38G.

References

Armstrong, J., & Leovy, C. (2005). Long term wind erosion on Mars. *Icarus*, *176*(1), 57–74. https://doi.org/10.1016/j.icarus.2005.01.005

Ayoub, F., Avouac, J.-P., Newman, C. E., Richardson, M. I., Lucas, A., Leprince, S., & Bridges, N. T. (2014). Threshold for sand mobility on Mars calibrated from seasonal variations of sand flux. *Nature Communications*, *5*(1), 5096. https://doi.org/10.1038/ncomms6096

Banks M. E., Fenton L.K., Bridges N. T., Geissler P. E., Chojnacki M., Silvestro S., Zimbelman J. R. (2017). Patterns in mobility and modification of middle and high latitude Southern Hemisphere dunes. Paper presented at the 48th lunar and planetary science conference. Houston, TX, Abstract 2918.

Banks M. E., Geissler P. E., Bridges N. T., Russell P., Silvestro S., Chojnacki M., Zimbelman, J. R., et al. (2015). Emerging global trends in aeolian bedform mobility on Mars. Paper presented at the fourth international planetary dunes workshop: Integrating models, remote sensing, and field data. Houston, TX, Abstract 8036.

Banks M. E., Geissler, P. E., Bridges N. T., Silvestro S., & Zimbelman J. R. (2014). Preliminary global trends in aeolian bedform mobility on Mars. Paper presented at the 45th lunar and planetary science conference. Houston, TX, Abstract 2857.

Bourke, M. C., Edgett, K. S., & Cantor, B. A. (2008). Recent aeolian dune change on Mars. *Geomorphology*, *94*(1–2), 247–255. https://doi.org/10.1016/j.geomorph.2007.05.012

Bourke, M. C., Ewing, R. C., Finnegan, D., & McGowan, H. A. (2009). Sand dune movement in the Victoria Valley, Antarctica. *Geomorphology*, *109*(3–4), 148–160. https://doi.org/10.1016/j.geomorph.2009.02.028

Bridges, N., Geissler, P., Silvestro, S., & Banks, M. (2013). Bedform migration on Mars: Current results and future plans. *Aeolian Research*, *9*, 133–151. https://doi.org/10.1016/j.aeolia.2013.02.004

Bridges, N. T., Banks, M. E., Beyer, R. A., Chuang, F. C., Noe Dobrea, E. Z., Herkenhoff, K. E., Keszthelyi, L. P., et al. (2010). Aeolian bedforms, yardangs, and indurated surfaces in the Tharsis Montes as seen by the HiRISE camera: Evidence for dust aggregates. *Icarus*, *205*(1), 165–182. https://doi.org/10.1016/j.icarus.2009.05.017

Bridges, N. T., Bourke, M. C., Geissler, P. E., Banks, M. E., Colon, C., Diniega, S., et al. (2012). Planet-wide sand motion on Mars. *Geology*, *40*(1), 31–34. https://doi.org/10.1130/G32373.1

Brothers, S. C., & Kocurek, G. (2018). The transitional depositional environment and sequence stratigraphy of Chasma Boreale. *Icarus*, *308*, 27–41. https://doi.org/10.1016/j.icarus.2017.08.038

Byrne, S., Dundas, C. M., Kennedy, M. R., Mellon, M. T., McEwen, A. S., Cull, S. C., Daubar, I. J., et al. (2009). Distribution of mid-latitude ground ice on Mars from new impact craters. *Science*, *325*, 1674–1676. https://doi.org/10.1126/science.1175307

Chojnacki, M., Banks, M. E., & Urso, A. C. (2018a). Boundary condition control on high sand flux regions of Mars. Paper presented at the 49th *Lunar and Planetary Science Conference*, The Woodlands, TX, Abstract 2331.

Chojnacki, M., Banks, M., & Urso, A. (2018b). Wind-driven erosion and exposure potential at Mars 2020 rover candidate-landing sites. *Journal of Geophysical Research: Planets*, *123*, 468–488. https://doi.org/10.1002/2017JE005460

Chojnacki, M., Burr, D. M., & Moersch, J. E. (2014). Valles Marineris dune fields as compared with other Martian populations: Diversity of dune compositions, morphologies, and thermophysical properties. *Icarus*, *230*, 96–142. https://doi.org/10.1016/j.icarus.2013.08.018

Chojnacki, M., Burr, D. M., Moersch, J. E., & Michaels, T. I. (2011). Orbital observations of contemporary dune activity in Endeavor crater, Meridiani Planum, Mars. *Journal of Geophysical Research*, *116*, E00F19. https://doi.org/10.1029/2010JE003675

Chojnacki, M., Johnson, J. R., Moersch, J. E., Fenton, L. K., Michaels, T. I., & Bell, J. F. III (2015). Persistent aeolian activity at Endeavour crater, Meridiani Planum, Mars; new observations from orbit and the surface. *Icarus*, *251*, 275–290. https://doi.org/10.1016/j.icarus.2014.04.044

Chojnacki, M., Urso, A., Fenton, L. K., & Michaels, T. I. (2017). Aeolian dune sediment flux heterogeneity in Meridiani Planum, Mars. *Aeolian Research*, *26*, 73–88. https://doi.org/10.1016/j.aeolia.2016.07.004

Christensen, P. R., Engle, E., Anwar, S., Dickenshied, S., Noss, D., Gorelick, N., & Weiss-Malik, M. (2009) JMARS—A planetary GIS. Paper presented at the American Geophysical Union Fall Meeting, San Francisco, CA, Abstract IN22A-06.

Christensen, P. R., Jakosky, B. M., Kieffer, H. H., Malin, M. C., McSween, H. Y. Jr., Nealson, K., et al. (2004). The Thermal Emission Imaging System (THEMIS) for the Mars 2001 Odyssey mission. *Space Science Reviews*, *110*, 85–130. https://doi.org/10.1007/978-0-306-48600-5_3

Diniega, S., Hansen, C. J., Allen, A., Grigsby, N., Li, Z., Perez, T., & Chojnacki, M. (2017). Dune-slope activity due to frost and wind throughout the north polar erg, Mars. *Geological Society, London, Special Publications*. https://doi.org/10.1144/SP467.6

Dundas, C. M., Diniega, S., Hansen, C. J., Byrne, S., & McEwen, A. S. (2012). Seasonal activity and morphological changes in Martian gullies. *Icarus*, *220*(1), 124–143. https://doi.org/10.1016/j.icarus.2012.04.005

Ewing, R. C., & Kocurek, G. (2010). Aeolian dune-field pattern boundary conditions. *Geomorphology*, *114*(3), 175–187. https://doi.org/10.1016/j.geomorph.2009.06.015

Ewing, R. C., Peyret, A.-P. B., Kocurek, G., & Bourke, M. (2010). Dune field pattern formation and recent transporting winds in the Olympia Undae dune field, north polar region of Mars. *Journal of Geophysical Research*, *115*, E08005. https://doi.org/10.1029/2009JE003526

Feldman, W., Bourke, M., Elphic, R., Maurice, S., Bandfield, J., Prettyman, T., Diez, B., et al. (2008). Hydrogen content of sand dunes within Olympia Undae. *Icarus*, *196*(2), 422–432. https://doi.org/10.1016/j.icarus.2007.08.044

Feldman, W. C., Prettyman, T., Maurice, S., Plaut, J. J., Bish, D. L., Vaniman, D. T., Mellon, M. T., et al. (2004). Global distribution of near-surface hydrogen on Mars. *Journal of Geophysical Research*, *109*, E09006. https://doi.org/10.1029/2003JE002160

Fenton, L. K. (2006). Dune migration and slip face advancement in the Rabe crater dune field, Mars. *Geophysical Research Letters*, *33*, L20201. https://doi.org/10.1029/2006GL027133

Fenton, L. K., Carson, H. C., & Michaels, T. I. (2018). Climate forcing of ripple migration and crest alignment in the last 400 kyr in Meridiani Planum, Mars. *Journal of Geophysical Research: Planets*, *123*, 849–863. https://doi.org/10.1002/2017JE005503

Fenton, L. K., Chojnacki, M., & Michaels, T. I. (2015). Late Amazonian aeolian features, gradation, wind regimes, and sediment state in the vicinity of the Mars exploration rover opportunity, Meridiani Planum, Mars. *Aeolian Research*, *16*, 75–99. https://doi.org/10.1016/j.aeolia.2014.11.004

Fenton, L. K., & Hayward, R. K. (2010). Southern high latitude dune fields on Mars: Morphology, aeolian inactivity, and climate change. *Geomorphology*, *121*(1–2), 98–121. https://doi.org/10.1016/j.geomorph.2009.11.006

Fenton, L. K., & Richardson, M. I. (2001). Martian surface winds: Insensitivity to orbital changes and implications for aeolian processes. *Journal of Geophysical Research*, *106*(E12), 32,885–32,902. https://doi.org/10.1029/2000JE001407

Greeley, R., Skypeck, A., & Pollack, J. B. (1993). Martian aeolian features and deposits: Comparisons with general circulation model results. *Journal of Geophysical Research*, *98*(E2), 3183–3196. https://doi.org/10.1029/92JE02580

Gullikson, A. L., Hayward, R. K., Titus, T. N., Charles, H., Fenton, L. K., Hoover, R. H., & Putzig, N. E. (2018). Mars Global Digital Dune Database: Composition, thermal inertia, and stability, in *49th Lunar and Planetary Science Conference*, The Woodlands, TX, Abstract 2304.

Haberle, R. M., Joshi, M. M., Murphy, J. R., Barnes, J. R., Schofield, J. T., Wilson, G., Lopez-Valverde, M., et al. (1999). General circulation model simulations of the Mars pathfinder atmospheric structure investigation/meteorology data. *Journal of Geophysical Research*, *104*(E4), 8957–8974. https://doi.org/10.1029/1998JE900040

Haberle, R. M., Murphy, J. R., & Schaeffer, J. (2003). Orbital change experiments with a Mars general circulation model. *Icarus*, *161*(1), 66–89. https://doi.org/10.1016/S0019-1035(02)00017-9

Hansen, C. J., Bourke, M., Bridges, N. T., Byrne, S., Colon, C., Diniega, S., Dundas, C., et al. (2011). Seasonal erosion and restoration of Mars' northern polar dunes. *Science*, *331*(6017), 575–578. https://doi.org/10.1126/science.1197636

Hansen, C. J., Thomas, N., Portyankina, G., McEwen, A., Becker, T., Byrne, S., Herkenhoff, K., et al. (2010). HiRISE observations of gas sublimation-driven activity in Mars' southern polar regions: I. Erosion of the surface. *Icarus*, *205*(1), 283–295. https://doi.org/10.1016/j.icarus.2009.07.021

Hayward, R. K., Fenton, L. K., Tanaka, K. L., Titus, T. N., Colaprete, A., & Christensen, P. R. (2010). Mars Global Digital Dune Database: MC1. U.S. Geological Survey Open-File Report 2010–1170. http://pubs.usgs.gov/of/2010/1170/

Hayward, R. K., Fenton, L. K., & Titus, T. N. (2014). Mars Global Digital Dune Database (MGD^3): Global dune distribution and wind pattern observations. *Icarus*, *230*, 38–46. https://doi.org/10.1016/j.icarus.2013.04.011

Hayward, R. K., Fenton, L. K., Titus, T. N., Colaprete, A., & Christensen, P. R. (2012). Mars Global Digital Dune Database: MC-30. U.S. Geological Survey Open-File Report 2012– 1259. http://pubs.usgs.gov/of/2012/1259/

Hayward, R. K., Mullins, K. F., Fenton, L. K., Hare, T. M., Titus, T. N., Bourke, M. C., Colaprete, A., et al. (2007a). Mars Global Digital Dune Database: MC2–MC29: U.S. Geological Survey Open-File Report 2007-1158. http://pubs.usgs.gov/of/2007/1158/

Hayward, R. K., Mullins, K. F., Fenton, L. K., Hare, T. M., Titus, T. N., Bourke, M. C., Colaprete, A., et al. (2007b). Mars Global Digital Dune Database and initial science results. *Journal of Geophysical Research*, *112*, E11007. https://doi.org/10.1029/2007JE002943

Head, J. W., Mustard, J. F., Kreslavsky, M. A., Milliken, R. E., & Marchant, D. R. (2003). Recent ice ages on Mars. *Nature*, *426*(6968), 797–802. https://doi.org/10.1038/nature02114

Hoover, R. H., Robbins, S. J., Putzig, N. E., Fenton, L. K., Hayward, R., Riggs, J., & Courville, S. (2018). Examining thermal inertia of layered ejecta craters and southern hemisphere dunes on Mars. Paper presented at the *49th Lunar and Planetary Science Conference*, The Woodlands, TX, Abstract 1811.

Horgan, B. H. N., & Bell, J. F. III (2012). Seasonally active slipface avalanches in the north polar sand sea of Mars: Evidence for a wind-related origin. *Geophysical Research Letters*, *39*, L09201. https://doi.org/10.1029/2012GL051329

Howard, A. D. (2000). The role of aeolian processes in forming surface features of the Martian polar layered deposits. *Icarus*, *144*(2), 267–288. https://doi.org/10.1006/icar.1999.6305

Kahre, M. A., Murphy, J. R., & Haberle, R. M. (2006). Modeling the Martian dust cycle and surface dust reservoirs with the NASA Ames general circulation model. *Journal of Geophysical Research*, *111*, E06008. https://doi.org/10.1029/2005JE002588

Kocurek, G. (1998). Aeolian system response to external forcing factors—A sequence stratigraphic view of the Sahara region. In K. W. Glennie (Ed.), *Quaternary Deserts and Climatic Change* (pp. 325–337). Rotterdam, Netherlands: A.A. Balkema.

Kocurek, G., Carr, M., Ewing, R., Havholm, K. G., Nagar, Y. C., & Singhvi, A. K. (2007). White Sands dune field, New Mexico: Age, dune dynamics and recent accumulations. *Sedimentary Geology*, *197*(3–4), 313–331. https://doi.org/10.1016/j.sedgeo.2006.10.006

Kocurek, G., & Lancaster, N. (1999). Aeolian system sediment state: Theory and Mojave Desert Kelso dune field example. *Sedimentology*, *46*, 505–515. https://doi.org/10.1046/j.1365–3091.1999.00227.x

Kok, J. F. (2010). An improved parameterization of wind-blown sand flux on Mars that includes the effect of hysteresis. *Geophysical Research Letters*, *37*, L12202. https://doi.org/10.1029/2010GL043646

Laskar, J., Correia, A. C. M., Gastineau, M., Joutel, F., Levrard, B., & Robutel, P. (2004). Long term evolution and chaotic diffusion of the insolation quantities of Mars. *Icarus*, *170*(2), 343–364. https://doi.org/10.1016/j.icarus.2004.04.005

Malin, M. C., Bell, J. F., Cantor, B. A., Caplinger, M. A., Calvin, W. M., Clancy, R. T., Edgett, K. S., et al. (2007). Context Camera Investigation on board the Mars Reconnaissance Orbiter. *Journal of Geophysical Research*, *112*, E05S04. https://doi.org/10.1029/2006JE002808

Malin, M. C., Danielson, G. E., Ravine, M. A., & Soulanille, T. A. (1991). Design and development of the Mars observer camera. *International Journal of Imaging Systems and Technology*, *3*(2), 76–91. https://doi.org/10.1002/ima.1850030205

McEwen, A. S., Eliason, E. M., Bergstrom, J. W., Bridges, N. T., Hansen, C. J., Delamere, W. A., Grant, J. A., et al. (2007). Mars Reconnaissance Orbiter's High Resolution Imaging Science Experiment (HiRISE). *Journal of Geophysical Research*, *112*, E05S02. https://doi.org/10.1029/2005JE002605

McKee, E. D. (1979). Introduction to a study of global sand seas. In E. D. McKee (Ed.), *A Study of Global Sand Seas*, *US Geological Survey Professional Paper 1052* (pp. 1–20). Washington, DC: US Government Printing Office.

Mellon, M. T., Arvidson, R. E., Sizemore, H. G., Searls, M. L., Blaney, D. L., Cull, S., Hecht, M. H., et al. (2009). Ground ice at the Phoenix Landing Site: Stability state and origin. *Journal of Geophysical Research*, *114*, E00E07. https://doi.org/10.1029/2009JE003417

Mellon, M. T., Boynton, W. V., Feldman, W. C., Arvidson, R. E., Titus, T. N., Bandfield, J. L., Putzig, N. E., et al. (2008). A prelanding assessment of the ice table depth and ground ice characteristics in Martian permafrost at the Phoenix landing site. *Journal of Geophysical Research*, *113*, E00A25. https://doi.org/10.1029/2007JE003067

Middlebrook, W. D. (2015). Three-dimensional and multi-temporal dune-field pattern analysis in the Olympia Undae dune field, Mars. (Master's Thesis). Retrieved from OAKTrust Digital Repository. College Station, TX: Texas A&M University. http://oaktrust.library.tamu.edu/handle/1969.1/155559

Piqueux, S., Edwards, C. S., & Christensen, P. R. (2008). Distribution of the ices exposed near the south pole of Mars using Thermal Emission Imaging System (THEMIS) temperature measurements. *Journal of Geophysical Research*, *113*, E08014. https://doi.org/10.1029/2007JE003055

Portyankina, G., Hansen, C. J., & Aye, K. M. (2017). Present-day erosion of Martian polar terrain by the seasonal CO_2 jets. *Icarus*, *282*, 93–103. https://doi.org/10.1016/j.icarus.2016.09.007

Runyon, K. D., Bridges, N. T., Ayoub, F., Newman, C. E., & Quade, J. J. (2017). An integrated model for dune morphology and sand fluxes on Mars. *Earth and Planetary Science Letters*, *460*, 320–321. https://doi.org/10.1016/j.epsl.2016.12.026

Runyon, K. D., Bridges, N. T., & Newman, C. E. (2017). Martian sand sheet characterization and implications for formation: A case study. *Aeolian Research*, *29*(April), 1–11. https://doi.org/10.1016/j.aeolia.2017.09.001

Shao, Y., & Lu, H. (2000). A simple expression for wind erosion threshold friction velocity. *Journal of Geophysical Research*, *105*(D17), 22,437–22,443. https://doi.org/10.1029/2000JD900304

Silvestro, S., Fenton, L. K., Vaz, D. A., Bridges, N. T., & Ori, G. G. (2010). Ripple migration and dune activity on Mars: Evidence for dynamic wind processes. *Geophysical Research Letters*, *37*, L20203. https://doi.org/10.1029/2010GL044743

Silvestro, S., Vaz, D. A., Di Achille, G., Popa, I. C., & Esposito, F. (2015). Evidence for different episodes of aeolian construction and a new type of wind streak in the 2016 ExoMars landing ellipse in Meridiani Planum. *Journal of Geophysical Research: Planets*, *120*, 760–774. https://doi.org/10.1002/2014JE004756

Silvestro, S., Vaz, D. A., Ewing, R. C., Rossi, A. P., Fenton, L. K., Michaels, T. I., Flahaut, J., et al. (2013). Pervasive aeolian activity along rover Curiosity's traverse in Gale crater, Mars. *Geology*, *41*(4), 483–486. https://doi.org/10.1130/G34162.1

Silvestro, S., Vaz, D. A., Fenton, L. K., & Geissler, P. E. (2011). Active aeolian processes on Mars: A regional study in Arabia and Meridiani terrae. *Geophysical Research Letters*, *38*, L20201. https://doi.org/10.1029/2011GL048955

Silvestro, S., Vaz, D. A., Yizhaq, H., & Esposito, F. (2016). Dune-like dynamic of Martian aeolian large ripples. *Geophysical Research Letters*, *43*, 8384–8389. https://doi.org/10.1002/2016GL070014

Smith, D. E., Zuber, M. T., Frey, H. V., Garvin, J. B., Head, J. W., Muhleman, D. O., Pettengill, G. H., et al. (2001). Mars orbiter laser altimeter: Experiment summary after the first year of global mapping of Mars. *Journal of Geophysical Research*, *106*(E10), 23,689–23,722. https://doi.org/10.1029/2000JE001364

Sullivan, R., Arvidson, R., Bell, J. F. III, Gellert, R., Golombek, M., Greeley, R., Herkenhoff, K., et al. (2008). Wind-driven particle mobility on Mars: Insights from Mars Exploration Rover observations at "El Dorado" and surroundings at Gusev crater. *Journal of Geophysical Research*, *113*, E06S07. https://doi.org/10.1029/2008JE003101

Tanaka, K., Rodriguez, J. A. P., Skinner, J. A. Jr., Bourke, M. C., Fortezzo, C. M., Herkenhoff, K. E., Kolb, E. J., et al. (2008). North polar region of Mars: Advances in stratigraphy, structure, and erosional modification. *Icarus*, *196*(2), 318–358. https://doi.org/10.1016/j.icarus.2008.01.021

Telfer, M. W., Parteli, E. J. R., Radebaugh, J., Beyer, R. A., Bertrand, T., Forget, F., Nimmo, F., et al., & The New Horizons Geology, Geophysics and Imaging Science Theme Team‡ (2018). Dunes on Pluto. *Science*, *360*(6392), 992–997. https://doi.org/10.1126/science.aao2975

Thomas, P. (1982). Present wind activity on Mars—Relation to large latitudinally zoned sediment deposits. *Journal of Geophysical Research*, *87*(B12), 9999–10,008. https://doi.org/10.1029/JB087iB12p09999

Toigo, A. D., Lee, C., Newman, C. E., & Richardson, M. I. (2012). The impact of resolution on the dynamics of the Martian global atmosphere: Varying resolution studies with the MarsWRF GCM. *Icarus*, *221*(1), 276–288. https://doi.org/10.1016/j.icarus.2012.07.020

Ward, A. W., Doyle, K. B., Helm, P. J., Weisman, M. K., & Witbeck, N. E. (1985). Global map of aeolian features on Mars. *Journal of Geophysical Research*, *90*(B2), 2038–2056. https://doi.org/10.1029/JB090iB02p02038

Wilson, J. T., Eke, V. R., Massey, R. J., Elphic, R. C., Feldman, W. C., Maurice, S., & Teodoro, L. F. A. (2018). Equatorial locations of water on Mars: Improved resolution maps based on Mars Odyssey neutron spectrometer data. *Icarus*, *299*, 148–160. https://doi.org/10.1016/j.icarus.2017.07.028

Withers, P. (2012). Empirical estimates of Martian surface pressure in support of the landing of Mars Science Laboratory. *Space Science Reviews*, *170*(1-4), 837–860. https://doi.org/10.1007/s11214-012-9876-2

Zimbelman, J. R. (2000). Non-active dunes in the Acheron fossae region of Mars between the Viking and Mars global surveyor eras. *Geophysical Research Letters*, *27*(7), 1069–1072. https://doi.org/10.1029/1999GL008399